scientific reports

Check for updates

OPEN

Recovery of rare earth elements from european coal mining waste

Francisco Javier Iglesias Rodríguez[1], Pedro Riesgo Fernández[1]✉, Alicja Krzemień[2], Antonio Luis Marqués Sierra[1] & Granadina Álvarez González[3]

Rare earth elements (REEs) are strategic raw materials for clean-energy technologies and high-value industrial applications. In this context, coal waste has attracted increasing attention as a potential secondary resource within circular-economy strategies for European coal regions. This study evaluates fine coal-waste materials from three European mining regions within the framework of the GreenJOBS and CRMsDataSpace RFCS projects. Four samples were analysed: two Spanish hard-coal wastes from La Matona and El Batán, one Polish hard-coal waste, and one Slovenian lignite-related waste. Total REE concentrations were determined in bulk materials and in selected particle-size fractions. Weighted average total REE contents ranged from 159.72 ppm in El Batán to 221.89 ppm in La Matona, with values of 202.39 ppm and 217.98 ppm for the Polish and Slovenian samples, respectively. Among the investigated materials, La Matona showed the highest total REE content and was therefore selected for laboratory-scale physical separation, exploratory leaching, and mineralogical characterisation. However, gravity, magnetic, electrostatic, and flotation tests produced only negligible REE enrichment. Leaching with water and acetic acid was ineffective, whereas hydrochloric acid at 60 °C increased dissolved REE concentrations but did not achieve extraction levels suitable for practical recovery under the tested conditions. SEM–EDS and XRD analyses indicate that REEs occur as scarce, fine-grained phases closely associated with quartz- and aluminosilicate-rich matrices. This textural association explains the limited response to conventional beneficiation techniques and the relatively homogeneous REE distribution among particle-size fractions, in contrast to many coal-related materials reported in the literature. Overall, the results suggest that the studied European coal wastes cannot be considered straightforward substitutes for primary REE ores.

Keywords Rare earth elements, Coal waste, Coal tailings, Physical separation, Hydrometallurgy, Circular economy, GreenJOBS project, CRMsDataSpace project

Rare earth elements (REEs) comprise the 14 lanthanides, often grouped into light REEs (LREEs: La, Ce, Pr, Nd, Sm) and heavy REEs (HREEs: Eu, Gd, Tb, Dy, Ho, Er, Tm, Yb, Lu). Scandium (Sc) and yttrium (Y) are frequently included in REE studies as they occur in the same deposits and share similar chemical behaviour. Sc is generally grouped with LREEs based on atomic weight, whereas Y is commonly treated as an HREE because of its association with heavy lanthanides in natural systems.

REEs underpin a wide range of clean-energy and high-technology applications, including permanent magnets for wind turbines and electric vehicles, catalysts, phosphors, and advanced defence systems[1–3]. Owing to their economic importance and the concentration of supply in a small number of countries, particularly China, which poses a significant supply risk, REEs have repeatedly been classified as critical raw materials (CRMs) by the European Commission. The most recent assessment by the European Commission[4] confirms that both light and heavy REEs remain critical raw materials for the European Union and are also designated strategic raw materials under the proposed Critical Raw Materials Act[5].

The strategic importance of rare earth elements (REEs), together with the risks associated with their supply, has stimulated increasing efforts to identify alternative and unconventional resources[6]. Among these, coal and coal-related materials—including coal seams, coal preparation wastes, fly ash, and coal mine drainage—have attracted considerable attention as potential secondary sources of REEs. Numerous studies have documented anomalous enrichments of REEs and Y in coal-bearing systems worldwide, with average total REE concentrations of approximately 68.5 ppm in coal and 404 ppm in coal ash. The apparent enrichment observed in coal combustion products results from the concentration of the inorganic fraction during combustion,

[1]Institute of Space Sciences and Technologies of Asturias (ICTEA), University of Oviedo, Independencia 13, 33004 Oviedo, Spain. [2]Department of Extraction Technologies, Rockburst and Risk Assessment, Central Mining Institute—National Research Institute, Plac Gwarków 1, 40-166 Katowice, Poland. [3]Mining and Environmental Engineering and Project Engineering, University of Oviedo, Independencia 13, 33004 Oviedo, Spain. ✉email: priesgo@uniovi.es

while most of the organic matter is removed. Consequently, elemental concentrations reported on an ash basis are substantially higher than those expressed on a whole-coal basis and can be converted by considering the ash yield of the sample. For example, for a coal containing 10 wt.% ash, the concentration of a conservatively behaving element in the resulting ash is expected to be approximately ten times greater than its concentration in the corresponding whole coal, assuming negligible volatilization or losses during combustion. In agreement with these observations, Ketris and Yudovich[7] reported average total REE concentrations of 69–72 ppm in lignite and bituminous coals, increasing to 378–469 ppm in the corresponding coal ashes. Based on the economic potential of coal combustion products, Seredin and Dai[8] proposed that beneficial recovery of REEs generally requires concentrations of approximately 1000 ppm rare earth oxides (REO) in coal ash. They further suggested that this threshold may decrease to 800–900 ppm REO for ashes derived from coal seams thicker than 5 m, a criterion that has become widely recognized in the literature as the Seredin–Dai cut-off.

Subsequent work has generalised this criterion to coal-related materials with > 100 ppm REO on a whole-coal basis or > 1000 ppm (0.1 wt.%) REO on an ash basis, provided that the REEs can be concentrated to at least 2 wt.% in the final product[9]. These thresholds, widely adopted in recent reviews and USGS assessments[10], provide a pragmatic benchmark for distinguishing REE-enriched coal and coal wastes from "normal" coal.

Simultaneously, research by the U.S. Department of Energy[11,12] has demonstrated that coal cleaning and combustion by-products can enrich REEs relative to the run-of-mine coal, and that coal refuse, fly ash, and related streams could represent viable feedstocks for REE recovery, provided that suitable physical and chemical concentration processes are identified. This aligns with a broader international trend towards recovering critical metals from mining and industrial waste, with recent work indicating that, in some jurisdictions, a significant fraction of critical mineral demand could technically be met from mine tailings and processing residues if economic and technological barriers are overcome.

Several authors have highlighted mining waste as a potential secondary raw material resource, both to mitigate supply limitations of primary metals and to address existing knowledge gaps in tailings valorisation[13].

Within the EU, these developments intersect with the European Green Deal[14] and the just transition agenda[15]. The GreenJOBS project[16] and the CRMsDataSpace project, both funded by the Research Fund for Coal and Steel (RFCS), explicitly target the repurposing of end-of-life underground coal mines by combining renewable-energy deployment with circular-economy technologies based on fine coal waste, including the potential recovery of REEs. In this context, fine coal wastes stored in preparation-plant ponds and dumps are not only an environmental liability but also a possible low-grade REE resource.

REE mining investment studies have shown that project viability is strongly dependent on both the total REE grade and the distribution of individual elements, typically captured by a "basket price" metric that weights each element's price by its proportion in the ore. This concept has been applied to several advanced rare-earth projects, illustrating how heavy-rare-earth and critical-element enrichments (e.g., Dy, Tb, Nd, Pr) can compensate for modest grades while highlighting the projects' vulnerability to price volatility[17,18]. In parallel, recent work on transgenic time series and ARIMA-based forecasting has quantified the strong cyclic and anomalous behaviour of REE prices, underlining the importance of robust price forecasts in early-stage economic assessments[19].

Against this background, the present study focuses on coal waste as a potential source of REEs in Europe. It builds on analytical work conducted within GreenJOBS on fine coal wastes from three representative coal-mining regions (Spain, Poland and Slovenia).

The specific aims are: To quantify REE contents and distribution in bulk and size-classified fine coal wastes from four samples representing three European coal basins; To calculate REE basket prices based on current (August 2025) market prices to assess compositional attractiveness; To evaluate the response of selected coal waste to physical concentration (gravity, magnetic, electrostatic and flotation) and to exploratory leaching tests and; To discuss the findings in the broader context of REE mining investment, resource reporting and circular-economy strategies for coal regions.

Materials and methods

Sample origin and preparation

Four fine coal-waste samples were investigated. Two samples originate from a Spanish hard-coal basin, one from a Polish hard-coal operation and one from a Slovenian lignite mine, selected as case studies in GreenJOBS.

In Spain, one sample was collected from the El Batán coal preparation plant. This material, composed of sandstone, shale, conglomerate, clay and minor carbonate particles derived from the lithologies of the Central Asturian Coal Basin, retains a relatively high proportion of organic matter. For comparison, a second sample was obtained from historical tailings generated when the same preparation plant operated under standard coal-processing conditions. These tailings were deposited in a separate waste dump known as "La Matona", from which the sample takes its name.

In Poland, the sample was obtained from a coal preparation plant processing underground longwall hard coal. The fine waste consists predominantly of lithic fragments derived from the coal seams of the Upper Silesian Coal Basin, including sandstone, shale and clay, together with a small proportion of residual hard coal. This material was accumulated in a surface dump. Chemically, it is characterised by a predominance of silica and alumina, with notable contributions from iron- and potassium-bearing minerals, as well as minor amounts of calcium- and titanium-bearing phases; all other constituents occur only in trace quantities.

In Slovenia, the sample was collected from a lignite mining operation employing longwall top-coal caving. The fine waste originates from the separation of overburden and interburden materials associated with lignite extraction and was deposited in a dedicated waste dump. The material consists mainly of clay-rich and siliceous sediments characteristic of the regional stratigraphy, together with subordinate lignite particles. Its chemical composition reflects this mineralogical assemblage, with silica and alumina as the dominant oxides, accompanied by minor quantities of iron, calcium, magnesium and other trace components.

All samples were air-dried, homogenised and riffle-split to obtain representative sub-samples for chemical analysis, physical separation tests and mineralogical characterisation. For the Spanish samples, sufficient material was available to perform both bulk analysis and extensive beneficiation tests. For the Polish and Slovenian samples, the work focused on bulk chemistry and particle-size distribution of REEs.

To approximate the size fractions naturally produced in coal preparation plants, the material was sieved into four classes: > 2.0 mm (rejection), 2.0–0.5 mm, 0.5–0.1 mm and < 0.1 mm. REE analyses were performed on the three finest fractions and then combined to obtain weighted-average grades for each sample.

Chemical analysis and basket price calculation

Total REE contents in each size fraction were obtained within the GreenJOBS analytical programme using Super Trace DL Na_2O_2 by Inductively coupled plasma mass spectrometry – ICP-AES procedures for trace-element analysis, and fusion X-ray fluorescence – XRF for REE oxides. The resulting data are reported as total REEs in ppm (µg/g). The analytical ranges for the different beneficiation products are summarized in Table 1.

For each bulk sample, REO "basket prices" were calculated following the net-metal-revenue approach widely applied in REO project assessments[17,18,20]. The basket price (BP) is defined as:

$$BP = \sum_i (REO_i\% \times P_i)$$

where REO_i% is the mass fraction of each rare-earth oxide in the total REO content of the sample, and P_i is its market price (US$/kg).

For this study, oxide prices (US$/kg) for August 2025 were taken from different specialised market providers; Thulium (Tm) was excluded from the calculations owing to its extremely high and volatile prices.

Sc and Y were grouped as "Sc–Y" and LREO and HREO sub-totals were also calculated to facilitate comparison with the literature.

Mineral processing experiments

To assess REE behaviour during conventional mineral processing, a series of laboratory-scale physical separation tests was conducted using the La Matona sample. This sample was selected because it combined the highest REE concentration with a relatively high inorganic matter content, making it the most suitable candidate for evaluating the response of REE-bearing minerals to beneficiation processes. In addition, the amount of material available from La Matona was sufficient to perform the complete experimental programme, whereas the remaining samples were only available in quantities adequate for characterization. Consequently, the beneficiation and subsequent hydrometallurgical tests were restricted to La Matona. Although this limits the direct extrapolation of the processing results to the other samples, the selected material is considered representative of fine coal wastes with elevated mineral matter and REE contents.

Size classification

Using a sieve shaker, to approximate the size fractions naturally produced in coal preparation plants, the four samples were sieved into four classes: > 2.0 mm (rejection), 0.5–2.0 mm, 0.1–0.5 mm and < 0.1 mm.

Subsequent beneficiation tests were carried out only on the La Matona sample, as it exhibited the highest REE content. Each test employed size fractions appropriate for the corresponding equipment: 0.5–2.0 mm for the pulsation box; 0.1–0.5 mm for both the shaking table and high-voltage electrostatic separation; and < 0.1 mm for the Mozley multi-gravity separator and froth flotation.

Gravity separation

Three gravity-based devices were tested:

Code	Analytical range					
ME_MS89L (ppm)	Ce	0.20–25,000	La	0.08–25,000	Tb	0.01–25,000
	Dy	0.03–25,000	Lu	0.05–25,000	Tm	0.01–25,000
	Er	0.02–25,000	Nd	0.07–25,000	Y	0.20–25,000
	Eu	0.03–25,000	Pr	0.03–25,000	Yb	0.02–25,000
	Gd	0.03–25,000	Sc	0.01–25,000		
	Ho	0.01–25,000	Sm	0.04–25,000		
ME_XRF30 (%)	CeO_2	0.01–50	La_2O_3	0.01–50	Tb_4O_7	0.01–10
	Dy_2O_3	0.01–10	Lu_2O_3	0.01–10	Tm_2O_3	0.01–10
	Er_2O_3	0.01–10	Nd_2O_3	0.01–10	Y_2O_3	0.01–10
	Eu_2O_3	0.01–10	Pr_6O_{11}	0.01–10	Yb_2O_3	0.01–10
	Gd_2O_3	0.01–10	Sc_2O_3	0.01–10		
	Ho_2O_3	0.01–10	Sm_2O	0.01–10		

Table 1. Analytical ranges (ppm) for rare earth elements determined by inductively coupled plasma atomic emission spectrometry (ICP-AES).

1. *Pulsation box (jigging)* A fixed-screen box with a diaphragm generating pulsations, creating a fluidised bed in which denser particles migrate to the lower part and lighter particles remain near the top. During the test, the 947.10 g of material was subjected to pulsations for a period of 5 min, promoting particle stratification according to density. Feed: 0.5–2.0 mm, products: heavy and light fractions.
2. *Shaking table* A flat table with rapid backwards and slow forward motion, combined with cross-flow water. Fine, heavy particles concentrate near the riffles, while coarse, light particles are washed away. The test finished once the effective sample mass of 559 g had been fully processed and the surface of the shaking table was free of visible particles. Feed: 0.1–0.5 mm, products: dense, light and mixed fractions.
3. *Mozley multi-gravity separator (MMGS)* A laboratory device simulating spiral and drum behaviour, combining rotating drum and shaking motions. 850 g of sample with an equal mass of water was prepared as a homogeneous slurry by mixing. The separator was operated at 240 rpm with a wash-water flow rate of 3 l/min, and the slurry was gradually fed until the entire sample had been processed. Feed: < 0.1 mm, products: dense, light 1, light 2 and washings. Only the dense and light 1 fractions were analysed, as these are the most relevant for continuous operation.

REE contents were measured across all relevant products to qualitatively estimate enrichment factors.

Magnetic separation
A high-intensity magnetic separator, with a feed current intensity of 3 A, corresponding to an approximate magnetic field strength of 20,000 Gauss, and a roller rotational speed of 20 rpm, was used to treat selected gravity concentrates from La Matona (0.5–2.0 mm and 0.1–0.5 mm). The aim was to exploit any paramagnetic behaviour of REE-bearing minerals. The dense concentrates were passed through the separator, producing magnetic and non-magnetic fractions, which were analysed for REEs.

Electrostatic separation
Electrostatic separation was carried out using a CARPCO Inc. EHTP 111–15 corona electrostatic separator operating at 30–40 kV and a drum rotation speed of 100 rpm. A feed size fraction of 0.1–0.5 mm was selected to ensure efficient particle charging and separation. The process relies on differences in the electrical conductivity and surface charging behaviour of the mineral phases present in the sample. Particles exhibiting higher conductivity were discharged rapidly and collected as the conductive fraction, whereas less conductive particles followed a different trajectory and reported to the non-conductive fraction. An intermediate mixed fraction was also collected. All products were subsequently analysed to evaluate the distribution of rare earth elements among the separated streams.

Froth flotation
Froth flotation tests were conducted on the < 0.1 mm fraction of La Matona, on the basis that REE-bearing minerals might be rendered selectively hydrophobic. A standard laboratory flotation cell was used, processing 200 g of sample mixed with water and agitated at 1250 rpm. Kerosene was employed as the collector (two drops) and the pulp was conditioned for 5 min, followed by the addition of two drops of methyl isobutyl carbinol (MIBC) as frother and a further 1 min of conditioning. Air was then introduced to initiate flotation, allowing hydrophobic particles to attach to air bubbles and report to the froth product. The test was continued until flotation exhaustion was reached, as indicated by the cessation of stable froth formation. Products were classified as froth (concentrate) and tailings, and subsequently analysed for REEs.

Ash yield determination

Ash yield was determined for all products obtained from the preparation and beneficiation tests performed on the La Matona coal mining waste (CMW) in accordance with the IGM-DE 004/87 standard method. Ash yield, defined as the mass of incombustible residue remaining after complete combustion under controlled conditions, is a key parameter for evaluating the mineral matter content of coal-derived materials and for expressing elemental concentrations on an ash basis. A total of 50 subsamples, including the raw sample and products obtained by sieving, pulsating jig, magnetic and electrostatic separation, shaking table, froth flotation, and Multi-Gravity Separator (MGS) tests, were analyzed. Prior to the analysis, all samples were ground to a particle size of < 20 µm to ensure sample homogeneity and complete combustion.

For each determination, approximately 1 g of homogenized sample was weighed into a pre-weighed porcelain crucible and combusted in a forced-air muffle furnace using a controlled heating program, with the temperature gradually increased to 700–750 °C and maintained for a total test duration of 4 h. After cooling in a desiccator to room temperature, the crucibles were reweighed, and the ash yield was calculated as the percentage of incombustible residue relative to the initial sample mass according to Eq. (4): Ash yield (%) = $[(A - B)/C] \times 100$, where A is the mass of the crucible containing the ash residue, B is the mass of the empty crucible, and C is the initial sample mass.

Hydrometallurgical concentration tests

Exploratory leaching (lixiviation) tests were performed on La Matona (< 0.1 mm) to assess the solubility of REEs under simple hydrometallurgical conditions. In all cases, 50 g of sample was mixed with 500 mL of solution (solid loading 100 g/L) and agitated for up to 24 h.

Three leaching media were tested:

1. **Distilled water** (21 °C, 24 h).
2. **1 N HCl** in distilled water at 21 °C and 60 °C, with contact times of 3, 6, 12 and 24 h.

3. **1 N CH_3COOH** (acetic acid) in distilled water at 21 °C and 60 °C, with the same contact-time schedule.

Leachates were analysed for dissolved REEs (ppb level), and trends in dissolution with time and temperature were evaluated qualitatively.

Mineralogical and microanalytical characterisation

The mineralogical and microanalytical characterisation of the La Matona sample was performed using scanning electron microscopy coupled with energy-dispersive X-ray spectroscopy (SEM–EDS) and X-ray diffraction (XRD).

For SEM–EDS, polished mounts were coated with a conductive gold layer and imaged at magnifications as low as 10 µm. Point analyses and elemental mapping were used to identify REE-bearing grains and their textural context.

Bulk mineralogy was determined by X-ray diffraction (XRD) using powdered specimens. Diffractograms were interpreted to identify major and minor crystalline phases. Quantitative phase proportions were estimated by normalising to 100% of crystalline material.

Once the mineral phases present had been identified and characterised, the mineral processing experiments described in this study were designed and established on the basis of the obtained mineralogical information.

Results

REE contents and size distribution

The REE contents for the four samples—La Matona and El Batán (Spain), Poland, and Slovenia—are presented in Fig. 1. Weighted average total REE concentrations range from approximately 160 to 222 ppm (0.016–0.022 wt%), with values of 221.89 ppm for La Matona, 159.72 ppm for El Batán, 202.39 ppm for the Polish sample, and 217.98 ppm for the Slovenian material.

As observed, the total REE contents are broadly similar across the four samples. Notably, the Spanish materials exhibit lower concentrations of Y, La, Gd, and Er than the Polish and Slovenian samples. Additionally, the El Batán sample contains markedly less Sc than the other three materials.

The samples were then divided into particle-size fractions: > 2.0 mm (rejection), 0.5–2.0 mm, 0.1–0.5 mm, and < 0.1 mm, as these sizes are obtained at various process points in a coal preparation plant (Fig. 2). The machines used were a jaw crusher, a disc mill, a sieve shaker with 0.1 mm, 0.5 mm and 2.0 mm sieves, and desamplers. REE analyses were performed on the three finest fractions and combined to obtain weighted average grades for each sample.

Table 2 presents the total REE contents for the three analysed size fractions of the La Matona (Spain) sample, yielding a weighted average of 221.89 ppm (0.022%). Overall, the fractions show no substantial differences in REE concentration. However, the 0.1–0.5 mm fraction exhibits slightly lower values for most REEs, except for Sc, which remains comparable to the other size classes.

The quantitative analysis results for the La Matona (Spain) sieved samples, expressed in parts per million, are presented in Fig. 3.

Table 3 presents the total REE contents for the three analysed size fractions of the El Batán (Spain) sample, yielding a weighted average of 159.72 ppm (0.016%). These values are lower than those obtained for the La Matona sample, likely due to the higher proportion of organic coal in El Batán. The quantitative analysis did not reveal any notable differences among the fractions.

Table 4 presents the total REE contents for the three analysed size fractions of the Polish sample, yielding a weighted average of 202.39 ppm (0.020%). As observed in the Spanish samples, the intermediate fraction shows slightly lower concentrations of most REEs, except for Sc, Pr, and Tb, which remain comparable to or slightly higher than in the Spanish samples.

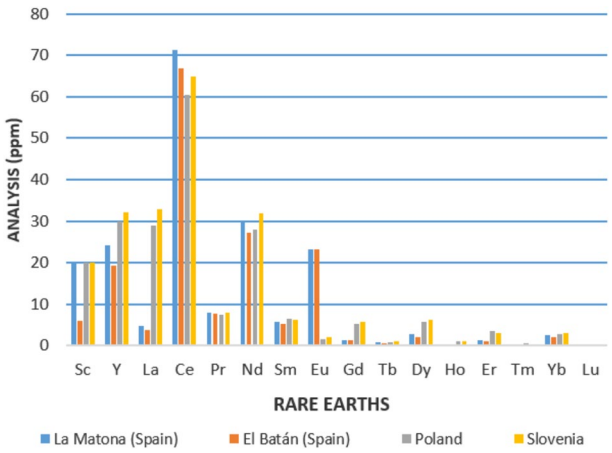


Fig. 1. Quantitative analysis of REEs (ppm) in samples from La Matona and El Batán (Spain), Poland, and Slovenia.



Fig. 2. Granulometric fractions of the La Matona sample: > 2.0 mm (top left), 2.0–0.5 mm (top right), 0.1–0.5 mm (bottom left), and < 0.1 mm (bottom right).

Sieve (mm)	Weight (%)	REEs (ppm)
0.5–2.0	38.83	231.98
0.1–0.5	27.15	204.74
< 0.1	9.93	229.35
Rejection > 2.0	24.09	–
Total	**100.00%**	**221.89**

Table 2. Granulometric fractions and corresponding REE contents of the La Matona (Spain) sample.

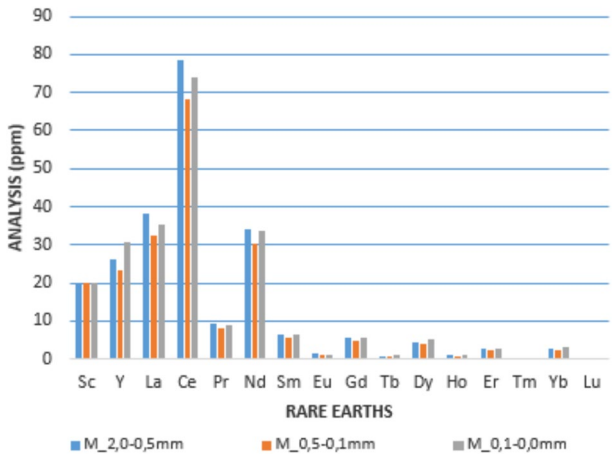


Fig. 3. Quantitative analysis results for the La Matona (Spain) sieved samples.

Sieve (mm)	Weight (%)	REEs (ppm)
0.5–2.0	41.07	165.13
0.1–0.5	21.01	148.97
< 0.1	4.17	160.63
Rejection > 2.0	33.75	–
Total	**100.00**	**159.72**

Table 3. Granulometric fractions and corresponding REE contents of the El Batán (Spain) sample.

Sieve (mm)	Weight (%)	REEs (ppm)
0.5–2.0	45.99	205.54
0.1–0.5	22.45	190.97
< 0.1	11.45	212.11
Rejection > 2.0	20.10	–
Total	100.00	**202.39**

Table 4. Granulometric fractions and corresponding REE contents of the Polish sample.

Sieve (mm)	Weight (%)	REEs (ppm)
0.5–2.0	13.91	228.21
0.1–0.5	31.66	236.26
< 0.1	27.50	191.75
Rejection > 2.0	26.93	–
Total	100.00	**217.98**

Table 5. Granulometric fractions and corresponding REE contents of the Slovenian sample.

Table 5 presents the total REE contents for the three analysed size fractions of the Slovenian sample, yielding a weighted average of 217.98 ppm (0.022%). In this case, the finest fraction shows lower concentrations for all REEs except Sc, a trend that may be related to dilution effects associated with the gypsum present in the sample.

The relatively homogeneous distribution of REEs across the different size fractions is an important finding, as it does not follow the general trend reported in the literature, where REEs are often preferentially enriched in the finest fractions. In the present case, the limited variation between particle-size classes suggests that REE distribution is not controlled solely by grain size or by the concentration of liberated fine particles.

Basket price composition

Basket price calculations for REO (Table 6) show notable differences among the studied samples, largely influenced by the relative proportions of Sc–Y and HREO. Using updated market prices representative of the 2026 rare-earth oxide market, the calculated basket prices are approximately 88.76 US$/kg for La Matona, 42.26 US$/kg for El Batán, 98.40 US$/kg for the Polish sample and 93.90 US$/kg for the Slovenian material. These values were calculated using current industrial market prices for individual rare-earth oxides, including updated benchmark quotations for terbium oxide (Tb_4O_7) and lutetium oxide (Lu_2O_3), obtained from specialized rare-earth market intelligence services [21–23]. Thulium oxide (Tm_2O_3) was excluded from the calculations due to the limited availability of reliable market quotations and its exceptionally high and volatile market value. Accordingly, the total rare earth oxide (REO) distribution was normalized on a Tm-free basis.

Across the four samples, the Sc–Y group averages 18.21% of the total REO content, with El Batán at the lower end (3.58%) and the Polish and Slovenian samples both exceeding 24%. Light rare-earth oxides (LREO) account for approximately 69.51% of the total REO assemblage on average, with El Batán exhibiting the highest proportion (76.90%). Heavy rare-earth oxides (HREO) contribute around 12.28% overall, reaching 19.52% in El Batán as a consequence of its lower Sc–Y content. Although HREO represent a smaller fraction of the total rare-earth inventory, they exert a disproportionately large influence on basket price because several heavy rare-earth oxides, particularly Tb_4O_7 and Lu_2O_3, command significantly higher market values than most light rare-earth oxides[21–23].

The basket price values are not directly comparable to those reported for hard-rock rare-earth projects, which generally refer to projected product streams after metallurgical recovery, upgrading and separation, and commonly range between 20 and 60 US$/kg REO in feasibility studies based on historical price assumptions[17,18]. Nevertheless, basket prices provide a useful indicator of the relative economic quality of a rare-earth assemblage because they integrate both elemental composition and market value. In this respect, the Polish and Slovenian samples combine moderate total REE concentrations with relatively high proportions of Sc, Y and HREEs, resulting in higher basket prices than those obtained for La Matona and, particularly, El Batán. These results

REO	Oxides US$/kg	La Matona	El Batán	Poland	Slovenia
Sc_2O_3	642.22	9.01%	2.30%	9.88%	9.18%
Y_2O_3	49.87	11.64%	1.28%	14.70%	14.84%
Total Sc_2O_3-Y_2O_3		**20.65%**	**3.58%**	**24.58%**	**24.02%**
La_2O_3	0.89	16.17%	18.18%	14.01%	14.77%
CeO_2	2.11	33.46%	38.76%	30.51%	29.83%
Pr_6O_{11}	64.74	3.95%	11.96%	2.73%	3.61%
Nd_2O_3	76.32	14.68%	7.01%	13.80%	14.38%
Sm_2O_3	1.95	2.72%	0.99%	3.35%	3.16%
Total LREO		**70.98%**	**76.90%**	**64.40%**	**65.75%**
Eu_2O_3	24.32	0.55%	0.85%	0.81%	0.80%
Gd_2O_3	23.46	2.40%	2.58%	2.76%	2.71%
Tb_4O_7	804.00	0.36%	0.45%	0.46%	0.47%
Dy_2O_3	237.93	1.99%	2.01%	2.97%	2.72%
Ho_2O_3	71.81	0.42%	0.44%	0.51%	0.48%
Er_2O_3	44.64	1.15%	1.13%	1.72%	1.37%
Tm_2O_3	–	0.17%	0.35%	0.20%	0.23%
Yb_2O_3	13.23	1.17%	11.54%	1.37%	1.28%
Lu_2O_3	707.00	0.16%	0.17%	0.22%	0.17%
Total HREO		**8.37%**	**19.52%**	**11.02%**	**10.23%**
Basket price US$/kg	–	**88.76**	**42.26**	**98.40**	**93.90**

Table 6. Basket price calculations.

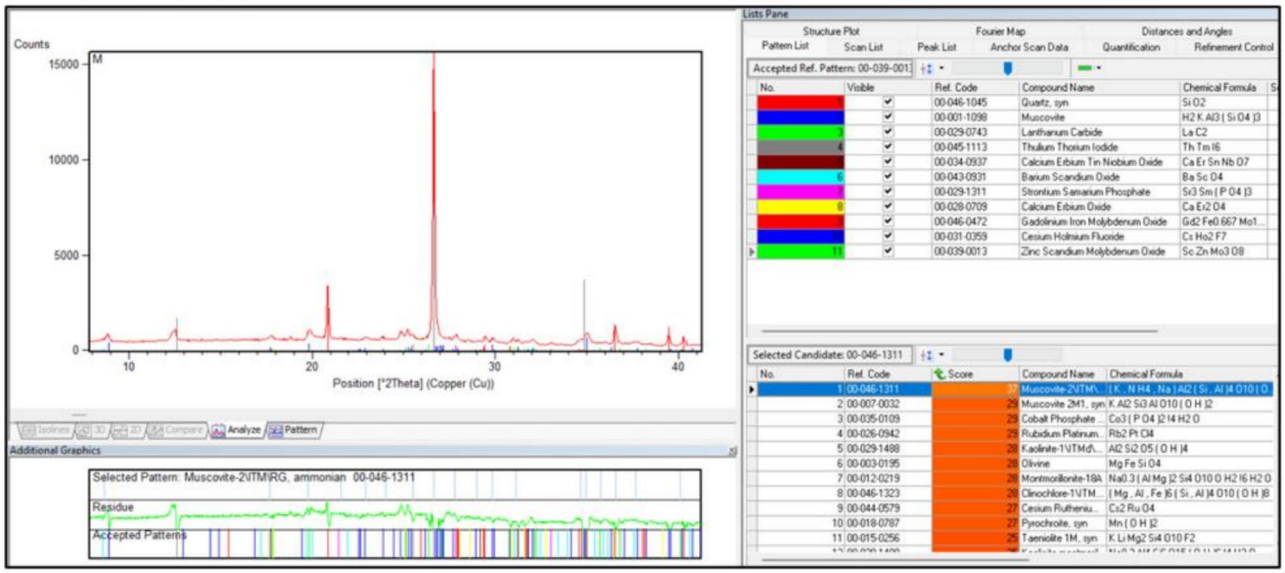


Fig. 4. X-ray diffraction (XRD) analysis of the La Matona sample.

highlight the importance of REE distribution and market weighting in the economic assessment of secondary rare-earth resources.

X-ray diffraction (XRD)

X-ray diffraction (XRD) was used to determine the crystalline mineral phases present in the La Matona sample. This technique is based on the interaction between incident X-rays and the ordered atomic structure of crystalline materials, producing diffraction patterns that are characteristic of each mineral phase. The resulting diffractogram allows identification of major and minor crystalline compounds based on their diagnostic peaks.

The XRD results for the La Matona sample are presented in Fig. 4. The diffraction pattern is dominated by quartz (SiO_2) and muscovite, together with other common aluminosilicate and carbonate minerals. Automated phase-search routines returned tentative matches with several REE-bearing reference patterns; however, none of these phases could be confirmed by quantitative phase analysis or refinement. Considering the weak and

overlapping diffraction peaks, the expected trace abundance of REEs, and the lack of geological evidence for discrete REE minerals in this type of coal waste, these matches are interpreted as artefacts of the automated pattern-matching procedure rather than as evidence for the presence of crystalline REE-bearing phases.

Table 7 presents the quantitative XRD results, normalised to 100%, which represent the relative proportions of the crystalline phases identified in the sample. As the material accumulated in the dump is mainly composed of sandstone, quartzite, shale, conglomerates and minor limestone, the mineralogical assemblage is dominated by phases typically associated with these lithologies. The main minerals identified include quartz, zeolite-group minerals such as pollucite, pyrite, calcite, dolomite, aragonite, fluorite, braunite, loparite and hercynite.

The qualitative XRD interpretation shown in Fig. 4 is consistent with the quantitative phase analysis presented in Table 6. The diffraction pattern is dominated by quartz and muscovite–illite group minerals, which together account for more than half of the crystalline material in the sample. Other significant phases identified include kaolinite-group minerals, chlorite, calcite and minor amounts of feldspars, carbonates, sulphides and iron oxides. This mineral assemblage is consistent with the sandstone, quartzite, shale, conglomerate and minor limestone lithologies that constitute the La Matona waste dump. No REE-bearing minerals were identified as major or quantitatively significant phases by XRD, indicating that rare earth elements occur only in minor or trace concentrations. Consequently, any REE-bearing phases are likely present below the quantification limit of the technique and/or as very fine inclusions, intergrowths or coatings associated with the dominant quartz, clay minerals and aluminosilicates. These textural relationships suggest that REEs do not occur predominantly as free and independent mineral phases. Instead, their occurrence within composite particles is expected to hinder their liberation and separation during mineral beneficiation processes, as the behaviour of the particles is largely controlled by the host minerals. As a result, REE-bearing particles may be distributed among different processing products together with their host phases, reducing the selectivity and efficiency of the separation process[24,25].

Mineral processing experiments

Gravity concentration

For gravity separation to be meaningfully interpreted in terms of REE behaviour, it is first necessary to consider the mineralogical context of the sample, particularly the identification of REE-bearing phases versus REE-free gangue phases, as well as their respective densities. However, as demonstrated in the mineralogical characterisation, REEs in the La Matona sample do not occur as discrete, well-defined mineral phases but are instead present at trace levels, likely hosted within or associated with quartz, aluminosilicates and clay minerals as very fine inclusions, coatings or intergrowths. This textural occurrence implies that REEs are not present as liberated phases but are structurally incorporated into composite particles dominated by low-density gangue minerals. As a result, the effective density and separation behaviour of these particles are controlled by the host phases rather than by the REE-bearing components.

Under these conditions, gravity concentration cannot be expected to directly separate REE-bearing minerals, but rather to fractionate composite particles according to the density of their dominant mineral matrix. Consequently, any observed variations in REE distribution across gravity products should be interpreted in terms of the behaviour of composite particles rather than the liberation and separation of discrete REE minerals.

Consistent with the higher densities of many REE-bearing minerals, gravity separation using the pulsation box, shaking table and Mozley multi-gravity separator (MMGS) is expected to produce dense fractions enriched in REEs, while lighter fractions should be comparatively depleted. The extent of enrichment varies with both the device and the particle-size range treated, with the MMGS generally proving more effective for the finest material (< 0.1 mm) than either the pulsation box or the shaking table within their respective operational windows.

However, given initial REE grades of approximately 220 ppm in the La Matona sample, even a two- to three-fold increase in REE content would remain well below the 800–900 ppm threshold commonly cited for economically viable recovery from coal ash. Gravity separation is therefore better suited as a pre-concentration stage and for examining REE partitioning than as a stand-alone upgrading route.

Mineral or mineral group	Mass (%)
Clay mineral (smectite, vermiculite, and palygorskite)—zeolite (pollucite)	2
Chlorite	9
Kandite group (kaolinite)	13
Muscovite—illite	15
Pyrophyllite	1
Plagioclase	2
K-feldspar and/or rutile	1
Quartz	41
Calcite	11
Dolomite—ankerite	1
Siderite-type carbonate	1
Pyrite	1
Hematite	1

Table 7. Relative proportions of the crystalline material in the La Matona sample.

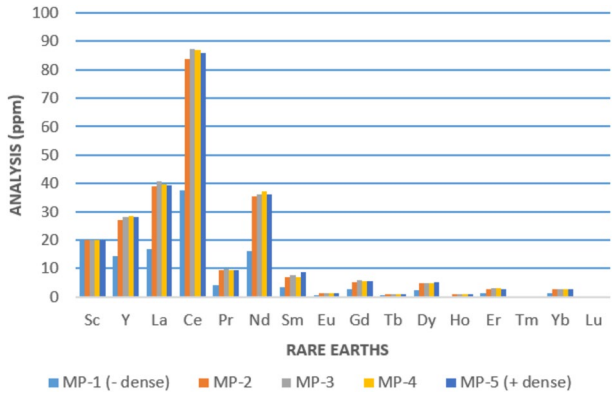


Fig. 5. Quantitative REE analysis (ppm) of the La Matona sample after separation using the pulsation box.

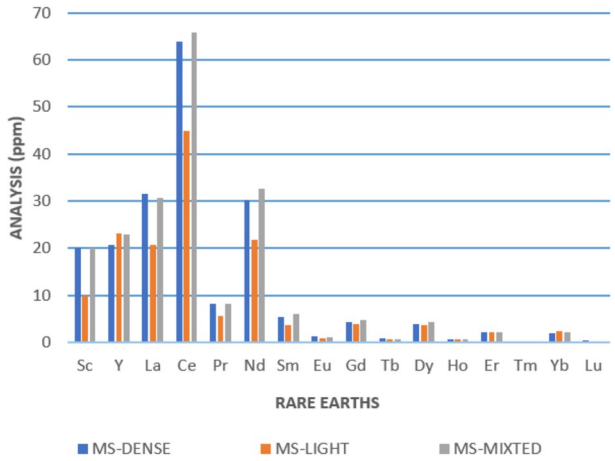


Fig. 6. Quantitative REE analysis (ppm) of the La Matona sample after separation using the shaking table.

The choice of equipment depends chiefly on the liberation characteristics of the material: the pulsation box is appropriate for particles between 0.5 and 2 mm, the shaking table for those between 0.1 and 0.5 mm, and the multi-gravity separator for material finer than 0.1 mm.

The pulsation box operates on the principle of differential acceleration and consists of a chamber fitted with a fixed screen, where pulsations generated by a diaphragm or piston induce alternating upward and downward accelerations. These pulsations, together with water introduced through several inlets, create a fluidised bed in which particles segregate according to density—lighter particles accumulating near the top of the bed and heavier particles migrating downward.

All products obtained from this device were subsequently analysed, and the resulting REE distributions are presented in Fig. 5. The results clearly show that the REEs tend to concentrate in the densest fractions, although only to a practically negligible extent. Consequently, the higher densities of many REE-bearing minerals do not exert a meaningful influence on the outcome of the gravity separation via the pulsation box.

The shaking table consists of a flat deck that undergoes a characteristic combination of rapid backwards and slow forward motions, enabling the separation of fine, dense particles from coarser and lighter ones. The fast backward stroke generates particle stratification by density, while the slower forward motion transports the pulp toward the discharge end of the table. As the material advances, the riffles gradually decrease in height, allowing the cross-flowing water to wash lighter, stratified particles toward the upper side of the deck, while heavier particles migrate toward the lower edge. The combined action of differential motion and water flow produces a fan-shaped distribution of minerals across the table surface, with well-defined zones where particles settle according to density.

This systematic separation yields dense, light and intermediate (mixed) fractions, the REE contents of which are presented in Fig. 6. In this case, a lower concentration of REEs is observed in the mixed fraction, while the dense and light fractions display practically similar concentrations. This outcome contradicts the expectation that the higher densities of many REE-bearing minerals would result in a measurable enrichment of REEs in the dense fraction.

The final gravity-based method applied was the Mozley multi-gravity separator (MMGS), a device that, at laboratory scale, reproduces the combined action of a Wenco drum and a shaking table typically used in

coal preparation plants. The MMGS separates the material into dense, light-1, light-2, and washing fractions; however, only the dense and light-1 products were analysed for REEs, as these are the fractions expected to be generated under continuous operating conditions. After drying, a total of 838.2 g of product was recovered. The mass distribution revealed that most of the material was concentrated in the Light-1 fraction (329.5 g), followed by the dense fraction (294.8 g), which together accounted for more than 74% of the total recovered mass (Fig. 6).

The results obtained using this method are presented in Fig. 7 . No significant enrichment of REEs was observed in any specific fraction. While certain elements show a slight tendency to concentrate in the dense product, others are marginally enriched in the light-1 fraction, indicating that the MMGS does not produce a clear density-based separation of REE-bearing phases in the studied material.

Magnetic concentration

Magnetic separation exploits differences in the magnetic susceptibility of minerals. In this study, the samples were subjected to high-intensity magnetic separation in order to assess whether REE-bearing phases could be selectively partitioned into magnetic or non-magnetic fractions. In mineral processing, magnetic separators are commonly used either to recover valuable magnetic minerals from gangue, such as magnetite from quartz, or to separate magnetic minerals from non-magnetic phases in complex ores, for example, in the recovery of wolframite or magnetite from cassiterite-bearing ores. Although all materials respond to a magnetic field to some extent, the response of many minerals is too weak to be of practical significance. Magnetic separation is also widely used in processing plants to remove metallic fragments that could damage equipment such as crushers and mills.

For optimal operation, the magnetic separator was applied to two particle-size fractions: 0.5–2.0 mm (153.0 g) and 0.1–0.5 mm (47.4 g). The products were separated into magnetic and non-magnetic fractions, and their REE contents are presented in Fig. 8. As observed in the previous separation tests, no clear REE enrichment was detected in either the magnetic or non-magnetic fraction for the 0.5–2.0 mm material. In the finer 0.1–0.5 mm fraction, REEs showed a slight tendency to concentrate in the non-magnetic product; however, this enrichment was too limited to be considered significant.

Electrostatic separation

High-voltage electrostatic separation was applied to the 0.1–0.5 mm fraction using a dry electric field of 30–40 kV and 100 rpm. This particle-size range was selected for operational reasons: coarser particles were too heavy to be effectively separated, whereas finer particles tended to adhere to the equipment and hinder the separation process. The method was considered appropriate because many REE-bearing minerals generally exhibit low electrical conductivity. Electrostatic separation exploits differences in electrical conductivity and surface charge among mineral particles. When exposed to an electric field, particles acquire a surface charge whose magnitude depends on their mineralogical composition and surface properties. Once charged, they can be separated through differential electrostatic attraction or repulsion.

The products obtained were classified into conductive, non-conductive and mixed fractions, and their REE contents are presented in Fig. 9. The results show only a very slight tendency for REEs to concentrate in the conductive fraction. However, this enrichment is negligible and therefore not significant.

Froth flotation

Froth flotation was performed on the < 0.1 mm fraction, which is the particle-size range most suitable for this method. This technique separates valuable minerals from non-valuable material by exploiting differences in their physicochemical surface properties, achieved by adding specific reagents. These reagents promote the attachment of hydrophobic particles to air bubbles at the liquid–gas interface, forming particle–bubble aggregates that rise to the pulp surface and are recovered as froth (Fig. 10).

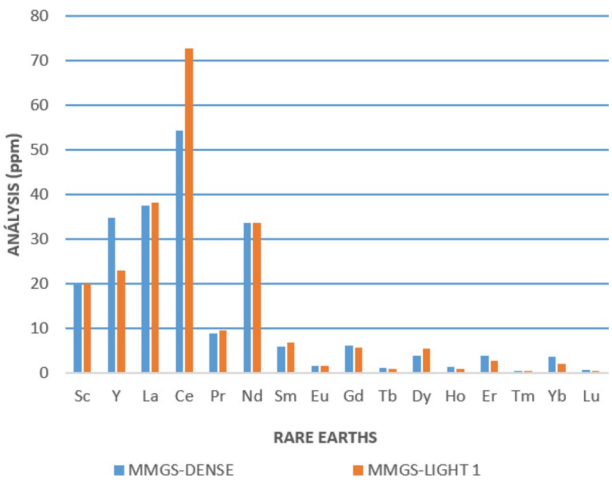


Fig. 7. Quantitative REE analysis (ppm) of the La Matona sample after separation using the Mozley multi-gravimetric separator.

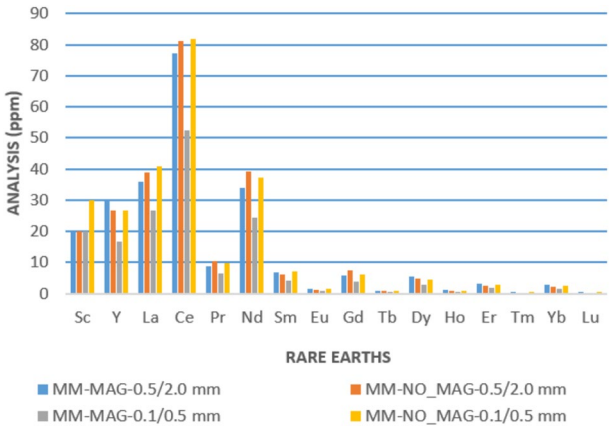


Fig. 8. Quantitative analysis of REEs (ppm) by magnetic field separation test in the La Matona sample.

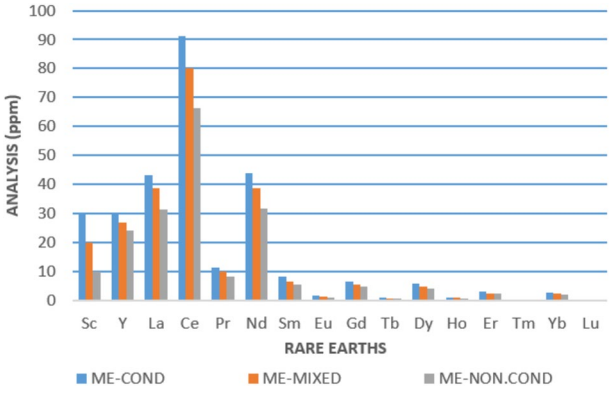


Fig. 9. Quantitative analysis of REEs (ppm) by the electric field separation test in the La Matona sample.

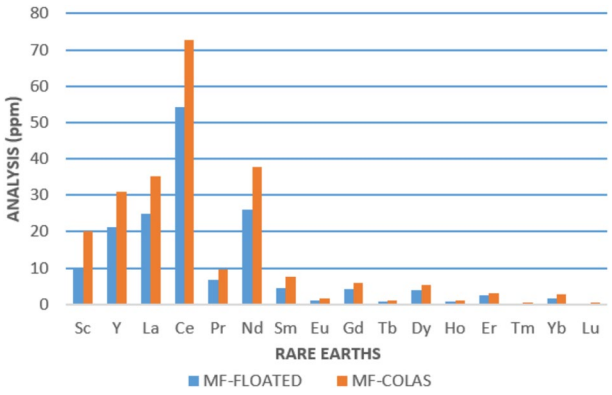


Fig. 10. Quantitative analysis of REEs (ppm) by the froth flotation test in the La Matona sample.

The products obtained from this test were divided into floated material and tailings, and their REE contents are presented in Fig. 10. Most of the material remained in the tailings fraction, accounting for approximately 93.7% of the recovered mass, whereas only 6.3% was recovered in the froth product. The results show a slight tendency for REEs to concentrate in the tailings; however, the degree of enrichment is negligible and therefore not significant.

Ash yield determination

Previous studies have reported a positive correlation between REE concentrations and ash yield in coal deposits, indicating that REEs are predominantly associated with the inorganic (mineral) fraction of coal rather than

with the organic matter[10]. This relationship is consistent with the enrichment of REEs in coal combustion products, where the removal of the organic fraction during combustion results in a proportional increase in the concentration of mineral-bound elements. Consequently, REE concentrations expressed on an ash basis provide a more appropriate framework for evaluating the economic potential of coal-derived materials and for comparison with the Seredin–Dai cut-off values proposed for REE recovery from coal ash (Seredin and Dai[8]).

Table 8 summarizes the REE concentrations, ash yields, and the corresponding theoretical REE concentrations in ash for all subsamples obtained from the beneficiation tests performed on the La Matona coal mining waste (CMW). The theoretical REE concentration in ash was calculated from the whole-sample REE concentration and the ash yield according to the following equation:

$$\text{Theoretical REE in ashes (ppm)} = [\text{REE in CMW (ppm)} / (\text{Ash yield (\%)} / 100)]$$

This calculation assumes conservative behavior of REEs during combustion, with negligible volatilization or elemental losses, as proposed by Xu et al. (2020).

The results are consistent with previous studies, confirming the close association of REEs with the mineral fraction of coal. Although high-density products exhibit the highest REE concentrations on a whole-sample basis, normalization to an ash basis reveals that the light fractions produced by gravity and flotation processes are relatively enriched in REEs, reaching theoretical concentrations of up to 429.8 ppm in ash. Despite remaining below the Seredin–Dai cut-off for economic recovery, these results demonstrate that physical beneficiation can effectively pre-concentrate REEs into selected mineral fractions, providing a suitable feedstock for subsequent extraction processes.

Hydrometallurgical concentration

Lixiviation with distilled water

A leaching test was carried out using 50 g of La Matona material with a particle size below 0.1 mm, mixed with distilled water to obtain a final solution volume of 500 mL. The suspension was stirred at room temperature for 24 h, and the resulting sample was labelled MW2124.

The results of this leaching test, expressed in parts per billion (ppb), are presented in Fig. 11. As shown, REE dissolution was negligible. For example, only 0.30 ppb of Sc was detected in the leachate, despite an initial Sc concentration of approximately 20 ppm in the solid sample.

Lixiviation with HCl

Leaching tests were carried out using 50 g of La Matona material with a particle size below 0.1 mm, mixed with a 1 N HCl solution prepared in distilled water to obtain a final volume of 500 mL. The tests were performed at two temperatures, 21 °C and 60 °C, and with agitation times of 3, 6, 12, and 24 h.

Sample	Description	REEs in CMW (ppm)	Ash Yield (%)	Theoretical REEs in Ash (ppm)
M-1	Raw sample	197.04	84.87	232.17
MT-1	Sieving (0.5–2.0 mm)	231.98	84.02	276.10
MT-2	Sieving (0.1–0.5 mm)	204.74	82.02	249.62
MT-3	Sieving (< 0.1 mm)	229.35	83.43	274.90
MP-1	Pulsating jig – Fraction 1 (low-density)	122.63	37.54	326.66
MP-2	Pulsating jig – Fraction 2	241.47	80.59	299.63
MP-3	Pulsating jig – Fraction 3	251.04	86.81	289.18
MP-4	Pulsating jig – Fraction 4	249.11	86.82	286.93
MP-5	Pulsating jig – Fraction 5 (high-density)	248.38	87.50	283.86
MS-D	Shaking table – Dense fraction	196.13	87.83	223.31
MS-L	Shaking table – Light fraction	144.54	43.23	334.35
MS-MIXED	Shaking table – Mixed fraction	202.91	74.15	273.65
MMGS-D	Multi-Gravity Separator (MGS) – Dense fraction	216.75	92.42	234.53
MMGS-L1	Multi-Gravity Separator (MGS) – Light fraction 1	223.06	72.63	307.12
MM-MAG-1	Magnetic separation (0.5–2.0 mm) – Magnetic fraction	234.23	84.57	276.97
MM-NO.MAG-1	Magnetic separation (0.5–2.0 mm) – Non-magnetic fraction	243.79	83.20	293.02
MM-MAG-2	Magnetic separation (0.1–0.5 mm) – Magnetic fraction	163.34	84.99	192.19
MM-NO.MAG-2	Magnetic separation (0.1–0.5 mm) – Non-magnetic fraction	253.96	79.03	321.35
ME-COND	Electrostatic separation – Conductive fraction	280.01	89.12	314.19
ME-MIXED	Electrostatic separation – Mixed fraction	240.56	85.75	280.54
ME-NO.COND	Electrostatic separation – Non-conductive fraction	194.26	72.67	267.32
MF-F	Froth flotation – Float product	162.93	37.91	429.78
MF-C	Froth flotation – Tailings	235.02	84.85	276.98

Tabla 8.. Relationship between REE content and ash yield in the La Matona subsamples.

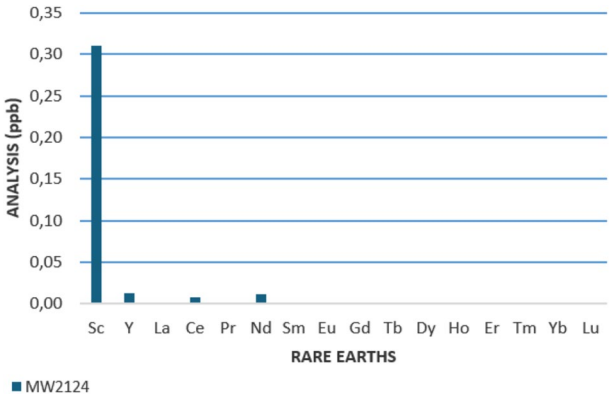


Fig. 11. Quantitative analysis of REEs (ppb) by lixiviation with water, at 21ºC and 24 h in the La Matona sample.

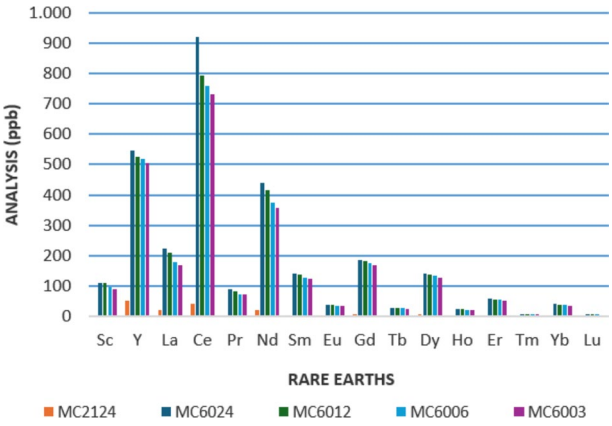


Fig. 12. Quantitative analysis of REEs (ppb) by lixiviation with a 1N solution of distilled water with HCl at different temperature and time conditions in the La Matona sample.

The results, expressed in parts per billion (ppb), are presented in Fig. 12. The data indicate that REE dissolution is influenced mainly by temperature rather than by agitation time. At 21 °C, no meaningful REE dissolution was observed, whereas at 60 °C, some elements showed slightly higher concentrations in the leachate. However, these concentrations remain very low and are insufficient to support the implementation of this hydrometallurgical route under the tested conditions.

Lixiviation with CH_3COOH

Leaching tests were carried out using 50 g of La Matona material with a particle size < 0.1 mm, mixed with a 1 N CH_3COOH solution prepared in distilled water to a final volume of 500 mL. The tests were conducted at two temperatures, 21 °C and 60 °C, and with agitation times of 3, 6, 12, and 24 h.

The results, expressed in parts per billion (ppb), are presented in Fig. 13. As observed, neither temperature nor agitation time produced significant differences in REE dissolution. Overall, the concentrations detected in the leachates were very low, indicating that, under the tested conditions, acetic acid does not promote meaningful REE extraction from the La Matona sample.

SEM–EDS

Scanning electron microscopy (SEM)

The La Matona sample was examined by scanning electron microscopy (SEM) to characterise its surface morphology and to identify representative areas for subsequent chemical analysis. Prior to observation, the material was dried, mounted on a sample holder and coated with a thin conductive gold layer to avoid charge accumulation during analysis (Fig. 14).

SEM imaging was performed at a scale of 10 µm, allowing the observation of particles with variable sizes, irregular shapes and locally agglomerated textures (Fig. 14). Three analytical points, labelled Spectrum 1, Spectrum 2, and Spectrum 3, were selected in different regions of the image to compare the chemical composition of contrasting microtextural areas.

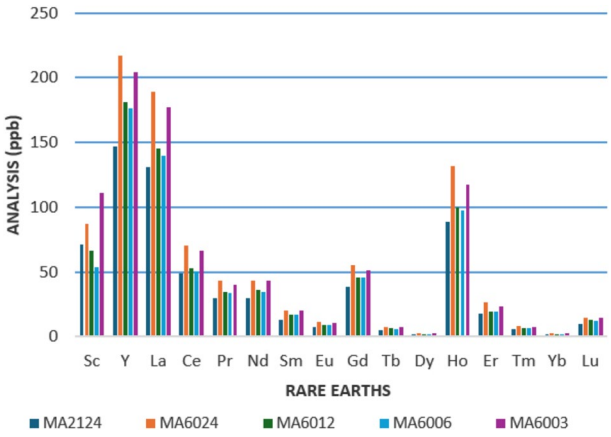


Fig. 13. Quantitative analysis of REEs (ppb) by lixiviation with a 1N solution of distilled water with CH3COOH at different temperature and time conditions in the La Matona sample.

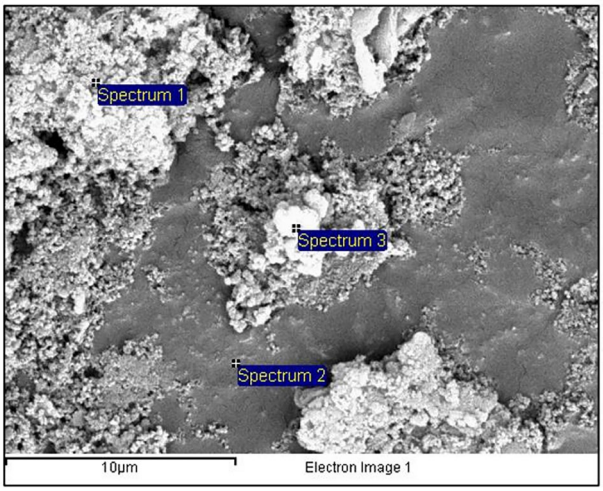


Fig. 14. Scanning electron microscopy (SEM) image of the La Matona sample.

X-ray energy dispersive spectrum (EDS)

SEM analysis was complemented by energy-dispersive X-ray spectroscopy (EDS), which enables chemical characterisation of selected points or areas within the SEM image. During EDS analysis, the electron beam excites the atoms in the sample, generating characteristic X-rays that are detected and used to determine the elemental composition. In this study, EDS analyses were performed on selected points of interest, labelled Spectrum 1, Spectrum 2 and Spectrum 3, to obtain elemental spectra and semi-quantitative chemical information from different regions of the La Matona sample.

Figure 15 shows the EDS spectrum obtained at Spectrum 1, from the SEM image in the previous section, covering an energy range up to 20 keV. The spectrum displays peaks associated with several rare-earth elements, including Y, Pr, Eu, Gd, Yb, and Lu. These results indicate the presence of REE-bearing phases within the analysed area and support the heterogeneous distribution of REEs observed in the SEM images.

According to these results, REEs do not appear to occur predominantly as free and independent mineral phases. Instead, they are likely present as very fine particles enclosed within or attached to other mineral phases, particularly quartz and aluminosilicates, or as intergrowths within these host minerals. These textural associations hinder their concentration and separation, since the behaviour of the composite particle during mineral beneficiation processes is largely controlled by the host mineral. Consequently, REE-bearing particles may be distributed among different products together with their host phases, thereby reducing the selectivity of the separation process[24,25].

The quantitative results show marked compositional differences among the three analysed points. This variability confirms the heterogeneous nature of the La Matona sample at the microscale.

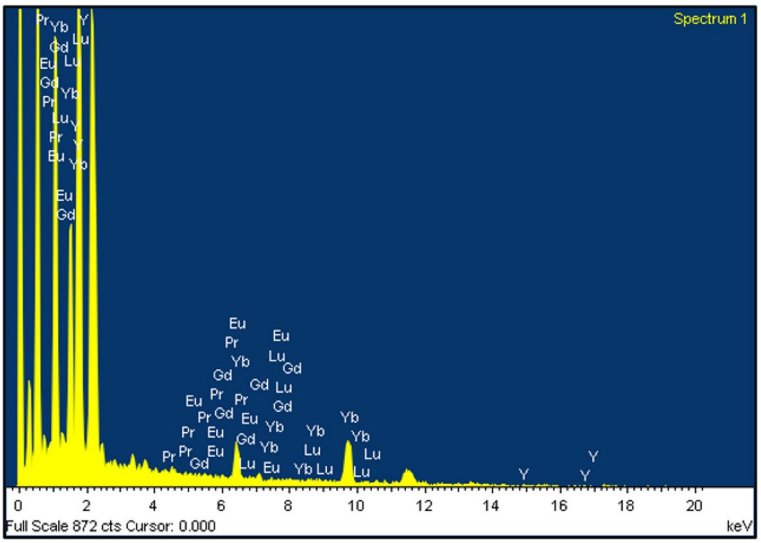


Fig. 15. X-ray energy dispersive spectrum (EDS) image of Spectrum 1.

Discussion and conclusions

The results confirm that fine coal wastes from the three evaluated European coal-mining regions contain measurable and persistent REE concentrations, but also show that grade alone is insufficient to define a recoverable resource. The weighted average contents of 159.72–221.89 ppm are higher than the normal world averages commonly reported for whole coal, and therefore justify considering these wastes in regional inventories of secondary raw materials. At the same time, they are well below the REO concentrations generally regarded as favourable for coal ash or coal-related feedstocks, especially the 800–1000 ppm ash-based benchmark and the requirement that beneficiation should produce a substantially enriched product.

A key observation is the relatively weak dependence of REE concentration on particle size. In many coal-related materials, REEs are preferentially associated with fine mineral matter, clay-rich fractions or combustion-derived ash phases. In the present samples, however, the three analysed size classes generally show only modest differences in total REE content. La Matona, for example, varies from 204.74 ppm in the 0.1–0.5 mm fraction to 231.98 ppm in the 0.5–2.0 mm fraction, while the Polish sample varies from 190.97 to 212.11 ppm. The Slovenian material is the main exception, with the finest fraction showing lower REE contents, probably reflecting dilution by mineral phases such as gypsum. This behaviour indicates that simple screening or desliming is unlikely to generate a preferentially enriched REE stream. For coal preparation plants, this is important because existing granulometric splits cannot be assumed to provide a direct upgrading route without more detailed knowledge of mineral liberation and host-phase associations.

The basket price calculation provides a useful compositional perspective that complements the total grade. The Polish and Slovenian samples show the highest calculated basket prices, at 99.53 and 95.05 US$/kg REO, despite having total REE contents similar to those of La Matona. This is mainly due to their higher proportions of Sc-Y and HREO, which are generally more valuable and more supply-constrained than the dominant low-priced LREO components. La Matona combines the highest total REE grade with a favourable but slightly lower basket price of 89.65 US$/kg REO, whereas El Batán has both the lowest grade and the lowest basket price, 43.36 US$/kg REO, largely because of its very low Sc and Y contribution. These differences underscore the need to assess coal-waste resources not only by total REE concentration but also by the distribution of critical elements.

The basket price values should not be interpreted as recoverable revenue. They do not account for mineral recovery, product purity, separation costs, penalties, reagent consumption, residue management or price volatility. This distinction is essential because REE projects are highly sensitive to the relative proportions of Nd, Pr, Dy, Tb, Sc, and Y, as well as to cyclical market behaviour. In the present case, the basket-price ranking is most valuable as an early-stage screening indicator. It suggests that the Polish and Slovenian wastes may be compositionally attractive for future characterisation, whereas La Matona is the most appropriate sample for process testing because it combines the highest total grade with sufficient material availability and a comparatively inorganic character.

Regarding physical separation, results show that conventional mineral-processing methods did not produce meaningful REE upgrading in the La Matona sample. Gravity concentration using a pulsation box, a shaking table, and a Mozley multi-gravity separator produced only minor and inconsistent partitioning of REEs between dense and light products. Magnetic separation also failed to generate a clear REE-rich fraction, although the finer 0.1–0.5 mm material showed a slight tendency for REEs to report to the non-magnetic product. Electrostatic separation gave only a weak enrichment in the conductive fraction, and froth flotation showed a slight tendency for REEs to remain in the tailings rather than in the floated material. These responses indicate that the behaviour of REE-bearing particles is controlled more by their host mineral particles than by the intrinsic density, magnetic susceptibility, conductivity or surface properties of individual REE minerals.

This interpretation is consistent with the mineralogical evidence. XRD indicates that La Matona is dominated by quartz, muscovite-illite, kaolinite, calcite and chlorite, with only minor phases containing REEs or associated metals. SEM–EDS confirms local REE-bearing areas but also reveals strong microscale heterogeneity. At the measured bulk grade of about 220 ppm, REE-bearing phases are necessarily scarce; if they occur as very fine inclusions, coatings or intergrowths within quartz and aluminosilicates, the composite particle will follow the physical properties of the host. This explains why dense, magnetic, conductive or hydrophobic products do not consistently concentrate REEs. It also aligns with the general beneficiation literature, which indicates that REE minerals require adequate liberation and carefully selected reagents or physical conditions for effective separation.

From a process-design perspective, these findings are significant. Even an idealised two- to three-fold enrichment of a 220 ppm feed would remain below the classical coal-ash threshold used to identify highly favourable REE feedstocks. The actual enrichment observed here is much smaller. Therefore, physical beneficiation alone cannot be considered a viable recovery route for La Matona under the tested conditions. Its more realistic role would be as a diagnostic or pre-concentration step, possibly combined with selective comminution, attrition, classification, removal of carbonaceous matter or targeting of specific mineral hosts once those hosts have been identified with higher-resolution mineralogical methods.

After developing physical separation, the exploratory leaching tests also indicate limited immediate extractability. Distilled water produced negligible REE dissolution, confirming that the REEs are not present in readily soluble salts or weakly adsorbed forms. Acetic acid did not generate a consistent or significant improvement, suggesting that carbonate dissolution or weak organic acid attack is insufficient to release the dominant REE inventory. HCl at 60 °C produced the greatest increase in dissolved REE concentrations; temperature was more influential than contact time, but the leachate concentrations remained in the ppb range. Under the tested solid loading, acid strength, and reaction times, this response is insufficient to support a practical leaching route.

The weak leaching response reinforces the interpretation that most REEs are locked within resistant mineral matrices or fine inclusions rather than occurring as readily exchangeable ions. *More aggressive treatments, such as stronger mineral acids, alkaline digestion, salt-assisted roasting, thermal activation, pressure leaching or bioleaching, might improve extraction, although their implementation should be supported by comprehensive techno-economic and environmental assessments before being considered viable for industrial application*[26]. This is particularly important for coal waste, where the principal advantage over primary mining should be the possibility of combining metal recovery with waste reduction, land rehabilitation and lower incremental disturbance. A process that requires high reagent consumption or creates problematic secondary residues could offset the circular-economy benefits that motivate this type of resource in the first place.

For Europe, the main value of the results lies in resource intelligence rather than immediate mine-scale extraction. The EU has identified both LREEs and HREEs as critical and strategic raw materials, and the European Critical Raw Materials Act emphasises domestic capacity, recycling and diversification of supply. Coal waste in Spain, Poland, Slovenia, and other coal regions is already mined and stored, and in many cases is environmentally problematic.

The present results argue against treating these materials as substitutes for primary REE ores. Their potential is more likely to emerge from integrated scenarios: reprocessing of waste during dump remediation, recovery of multiple elements, production of construction or backfill materials from cleaned residues, reduction of environmental liabilities and reuse of mining land and infrastructure.

Data availability

The datasets used and/or analysed during the current study are available from the corresponding author on reasonable request.

Received: 26 May 2026; Accepted: 13 July 2026
Published online: 29 July 2026

References

1. Elshkaki, A. & Graedel, T. E. Dysprosium, the balance problem, and wind power technology. *Appl. Energy* **136**, 548–559 (2014).
2. Fernandez, V. Rare-earth elements market: A historical and financial perspective. *Resour. Policy* **53**, 26–45. https://doi.org/10.1016/j.resourpol.2017.05.010 (2017).
3. Medeiros, FFd. et al. Rare earth elements: A review of primary sources, applications, business investment, and characterization techniques. *Appl. Sci.* **15**(20), 10949. https://doi.org/10.3390/app152010949 (2025).
4. European Commission. Study on the critical raw materials for the EU 2023: Final report. European Commission: Brussels, Belgium. 2023
5. European Parliament and the Council. European critical raw materials act. Regulation (EU) 2024/1252 of the European parliament and of the council of 11 April 2024 establishing a framework for ensuring a secure and sustainable supply of critical raw materials and amending regulations (EU) No 168/2013, (EU) 2018/858, (EU) 2018/1724 and (EU) 2019/1020. 2024
6. Binnemans, K. et al. Recycling of rare earths: A critical review. *J. Clean. Prod.* **51**, 1–22. https://doi.org/10.1016/j.jclepro.2012.12.037 (2013).
7. Ketris, M. P. & Yudovich, Y. E. Estimations of Clarkes for carbonaceous biolithes: World averages for trace element contents in black shales and coals. *Int. J. Coal Geol.* **78**(2), 135–148. https://doi.org/10.1016/j.coal.2009.01.002 (2009).
8 Seredin, V. V. & Dai, S. Coal deposits as potential alternative sources for lanthanides and yttrium. *Int. J. Coal Geol.* **94**, 67–93. https://doi.org/10.1016/j.coal.2011.11.001 (2012).
9. Eterigho-Ikelegbe, O., Harrar, H. & Bada, S. Rare earth elements from coal and coal discard: A review. *Miner. Eng.* **173**, 107187. https://doi.org/10.1016/j.mineng.2021.107187 (2021).
10. Scott, C. & Kolker, A. Rare earth elements in coal and coal fly ash: U.S. Geological survey fact sheet 2019–3048, pp. 4. 2019. https://doi.org/10.3133/fs20193048

11. U.S. Department of Energy. Recovery of rare earth elements and critical minerals from coal and coal byproducts: report to congress. U.S. Department of Energy, Washington, DC. 2022
12. U.S. Department of Energy. Report on rare earth elements from coal and coal byproducts: Report to congress. U.S. Department of energy, Washington, DC. 2017
13. Kretschmann, J., Efremenkov, A. B. & Khoreshok, A. A. From mining to post-mining: The sustainable development strategy of the German hard coal mining Industry. *IOP Conf. Ser. Earth Environ. Sci.* **50**, 012024. https://doi.org/10.1088/1755-1315/50/1/012024 (2017).
14. European Commission. Communication from the commission: The European green deal; COM(2019) 640 final, 11.12.2019; European commission: Brussels, Belgium. 2019
15. European Commission. Commission staff working document—performance, monitoring and evaluation of the european regional development fund, the cohesion fund and the just transition fund in 2021–2027, SWD(2021) 198 Final, 8.7.2021. European commission: Brussels; European commission: Brussels, Belgium, 2021.
16. Krzemień, A., Frejowski, A., Fidalgo Valverde, G., Riesgo Fernández, P. & Garcia-Cortes, S. Repurposing end-of-life coal mines with business models based on renewable energy and circular economy technologies. *Energies* **16**, 7617. https://doi.org/10.3390/en16227617 (2023).
17. Riesgo García, M. V., Krzemień, A., Manzanedo del Campo, M. Á., Menéndez Álvarez, M. & Gent, M. R. Rare earth elements mining investment: It is not all about China. *Resour. Policy* **53**(April), 66–76. https://doi.org/10.1016/j.resourpol.2017.05.004 (2017).
18. Riesgo García, P., Olías, M., Cerón, J. C. & Fernández, I. Economic evaluation and market outlook for rare earth element projects. *Miner. Eng.* **112**, 1–12 (2017).
19. Riesgo García, M. V., Krzemień, A., Manzanedo del Campo, M. Á., Escanciano García-Miranda, C. & Sçánchez Lasheras, F. Rare earth elements price forecasting by means of transgenic time series developed with ARIMA models. *Resour. Policy* **59**, 9–102. https://doi.org/10.1016/j.resourpol.2018.06.003 (2018).
20. Machacek, E. & Fold, N. Alternative value chains for rare earths: The Anglo-deposits developers. *Resour. Policy* **42**, 53–64. https://doi.org/10.1016/j.resourpol.2014.09.003 (2014).
21. Fastmarkets. Terbium oxide 99.99% CIP Global (MB-TB-0004): Rare Earths price assessment. fastmarkets metals and mining, London, UK. 2026
22. Lanthanides.io. Lutetium price 2026: Lu_2O_3 and metal market assessment. Lanthanides.io, Rare Earth Market Intelligence Database. 2026a
23. Lanthanides.io. Terbium price 2026: Tb_4O_7 and metal market assessment. Lanthanides.io, Rare Earth Market Intelligence database. 2026b
24. Jordens, A., Cheng, Y. P. & Waters, K. E. A review of the beneficiation of rare earth element bearing minerals. *Min. Eng.* **41**, 97–114. https://doi.org/10.1016/j.mineng.2012.10.017 (2013).
25. Weng, Z., Jowitt, S. M., Mudd, G. M. & Haque, N. A detailed assessment of global rare earth element resources: Opportunities and challenges. *Econ. Geol.* **110**(8), 1925–1952. https://doi.org/10.2113/econgeo.110.8.1925 (2015).
26. Yazici, E. Y. et al. Techno-economic and environmental assessntmes for hydrometallurgical treatment of waste lithium-ion batteries (LIBs): The ELiMINATE project. *Physicochem Probl Min Process* **61**(3), 204772. https://doi.org/10.37190/ppmp/204772 (2025).

Author contributions

Conceptualisation, A.K., F.J.I.R., A.L.M.S., and P.R.F.; methodology, A.K., and F.J.I.R. ; software, F.J.I.R.; validation, F.J.I.R. and A.L.M.S.; formal analysis, F.J.I.R. and A.L.M.S.; investigation, A.K., G.A.G., A.L.M.S. and P.R.F.; resources, G.A.G., A.K., and A.L.M.S.; data curation, F.J.I.R. and G.A.G.; writing—original draft preparation, G.A.G.; writing—review and editing, F.J.I.R. and G.A.G.; visualisation, G.A.G., and A.L.M.S.; supervision, F.J.I.R.; project administration, A.K. and P.R.F.; funding acquisition, A.K., A.L.M.S., and P.R.F. All authors have read and agreed to the published version of the manuscript.

Funding

The research presented in this paper was carried out as part of the GreenJOBS project (Leveraging the competitive advantages of end-of-life underground coal mines to maximise the creation of green and quality jobs), funded by the EU Research Fund for Coal and Steel (RFCS) under contract number 101057789, and with funding from the Polish Ministry of Education and Science under contract number 5275/FBWiS/2022/2023/2; and as part of the CRMsDataSpace project (Common European Data Space on Critical Raw Materials for the Green Deal: Recovery Potential from Closed Extractive Coal Waste Facilities), funded by the EU Research Fund for Coal and Steel (RFCS) under contract number 101216677, and with funding from the Polish Ministry of Education and Science under contract number XXXX/2026.

Declarations

Competing interests

The authors declare no competing interests.

Additional information

Correspondence and requests for materials should be addressed to P.R.F.

Reprints and permissions information is available at www.nature.com/reprints.

Publisher's note Springer Nature remains neutral with regard to jurisdictional claims in published maps and institutional affiliations.

Open Access This article is licensed under a Creative Commons Attribution 4.0 International License, which permits use, sharing, adaptation, distribution and reproduction in any medium or format, as long as you give appropriate credit to the original author(s) and the source, provide a link to the Creative Commons licence, and indicate if changes were made. The images or other third party material in this article are included in the article's Creative Commons licence, unless indicated otherwise in a credit line to the material. If material is not included in the article's Creative Commons licence and your intended use is not permitted by statutory regulation or exceeds the permitted use, you will need to obtain permission directly from the copyright holder. To view a copy of this licence, visit http://creativecommons.org/licenses/by/4.0/.

© The Author(s) 2026